IOPscience iopscience.iop.org

Home Search Collections Journals About Contact us My IOPscience

Magnetotransport in $(Ce_{1-x}Nd_x)Cu_6$ Kondo alloys

This article has been downloaded from IOPscience. Please scroll down to see the full text article.

1999 J. Phys.: Condens. Matter 11 2285

(http://iopscience.iop.org/0953-8984/11/10/015)

View the table of contents for this issue, or go to the journal homepage for more

Download details:
IP Address: 171.66.16.214
The article was downloaded on 15/05/2010 at 07:12

Please note that terms and conditions apply.

J. Phys.: Condens. Matter **11** (1999) 2285–2302. Printed in the UK PII: S0953-8984(99)98097-9

Magnetotransport in $(Ce_{1-x}Nd_x)Cu_6$ Kondo alloys

André M Strydom and Paul de V du Plessis

f-Electron Magnetism and Heavy-Fermion Physics Programme, Department of Physics, University of the Witwatersrand, Private Bag 3, PO WITS 2050, Johannesburg, South Africa

Received 5 October 1998

Abstract. The results of electrical resistivity $\rho(T)$ and magnetoresistivity MR(T, B) for $1.5 \leqslant T \leqslant 580$ K and $\mu_0 H = B \leqslant 8$ T are reported for the $(Ce_{1-x}Nd_x)Cu_6$ alloy system. For small Nd substitutions in the heavy-fermion $CeCu_6$ parent compound, the Kondo lattice is characterized through coherence effects in $\rho(T)$ at low temperatures. The $\rho(T)$ data above room temperature are used to resolve the electron–phonon scattering, and it is indicated that the single-ion Kondo interaction dominates both $\rho(T)$ and MR(B) for a wide range of intermediate Ce concentrations. Based on this, the MR(B) data for different isotherms and alloy compositions are analysed according to the Bethe-*ansatz* description. We also discuss the observed deviations of our data from the preceding theoretical description due to the onset of magnetic order in alloys with high Nd content, and to phase coherence at low temperatures.

1. Introduction

After its initial synthesis and study of electrical, magnetic and specific heat properties by Onuki *et al* [1] and Stewart *et al* [2], the heavy-fermion compound $CeCu_6$ continues to attract considerable attention. A review of many of its thermodynamic and transport properties, along with those of other $CeCu_x$ compounds ($x = 1, 2, 4, 5$ or 6), has been given by Bauer [3]. The RCu_6 compounds (R = La, Ce, Pr, Nd, Sm or Gd) all crystallize in the orthorhombic $CeCu_6$ *Pnma* structure at high temperatures [3, 4]. A continuous lattice-structural transformation takes place at temperature T_t to a low-temperature monoclinic ($P2_1/c$) structure [4] for $CeCu_6$ ($T_t = 230$ K), $LaCu_6$ ($T_t = 491$ K), $PrCu_6$ ($T_t = 216$ K) and $NdCu_6$ ($T_t = 155$ K). The monoclinic distortion is small however and generally the orthorhombic notation is conserved for simplicity when discussing their low-temperature properties.

Transport and thermodynamic properties of single-crystal $CeCu_6$ have been studied down to millikelvin temperatures by several authors [5–9]. These studies confirm the occurrence of a peak in the resistivity $\rho(T)$ at $\sim$10 K below which it drops precipitously and only attains a T^2 Fermi-liquid-like temperature dependence below 100 mK. It is noted that Sumiyama *et al* [9] observed a marked anisotropy in $\rho(T)$ in the millikelvin regime with only the a-axis resistivity conforming to the T^2-dependence while a $T^{2.07}$-dependence is observed for the c-axis and a $T^{1.71}$-dependence is found for the b-axis.

An electronic contribution to the specific heat at low temperature of $\gamma(T \rightarrow 0) = 1670$ mJ mol^{-1} K^{-2} is observed for $CeCu_6$ [7]. From de Haas–van Alphen measurements, effective field-dependent quasiparticle masses up to 80 times the free-electron mass are observed [10, 11]. The authors also conclude that mass enhancement of all the electrons involved near the Fermi surface takes place and not only of those of primarily f character [10]. Application of a large magnetic field significantly decreases the quasiparticle mass [11]

0953-8984/99/102285+18$19.50 © 1999 IOP Publishing Ltd

which is in agreement with a decrease of γ to 30% of its zero-field value when applying a field of 7.5 T [7]. Application of a magnetic field also increases the temperature regime in which a Fermi-liquid T^2-dependence of $\rho(T)$ is observed [7]. Earlier measurements of $\rho(T)$ down to 20 mK [8, 9] and specific heat $C(T)$ down to 60 mK [7, 12] indicate no evidence of magnetic ordering or superconductivity in $CeCu_6$. However, using inelastic neutron scattering, the existence of short-ranged magnetic correlations developing below 10 K was first indicated by Aeppli *et al* [13] and subsequently by Rossat-Mignod *et al* [14, 15]. The magnetic origin of the inelastic scattering is confirmed by the strong influence of a magnetic field on its intensity, being suppressed by an applied magnetic field of 2.5–4 T along the easy c-axis. Within the total magnetic scattering, contributions due to single-site and to antiferromagnetic correlations between adjacent 4f moments in the bc-plane could be resolved [14, 15]. The single-site fluctuations are associated with the Kondo interaction on localized Ce 4f moments and can be described by a quasi-elastic Lorentzian, the width of which yields a value of the Kondo temperature $T_K = 5 \pm 0.5$ K [14]. Muon-spin-rotation (μSR) measurements proved to be extremely useful in investigating possible small-moment magnetism in heavy-fermion systems [16]. Zero-field μSR measurements down to 40 mK show no sign of a magnetic transition and give an upper limit of $\simeq 10^{-3}\mu_B$/Ce atom for a static 4f moment [17].

Magnetic ordering can be obtained in $CeCu_6$ by doping. Thus for $Ce(Cu_{6-x}M_x)$ alloys (M = Au [18–20], Ag [18, 21, 22] or Pd [23]) antiferromagnetic ordering takes place above a critical concentration $x = x_c$ when the Rudermann–Kittel–Kasuya–Yosida (RKKY) interaction dominates the Kondo interaction. For $Ce(Cu_{6-x}Au_x)$, samples with the critical concentration $x_c = 0.1$ have been comprehensively studied and shown to exhibit non-Fermi-liquid behaviour which has been attributed to the suppression to $T = 0$ K of the magnetic order [24, 25]. Hence, it seems as if $CeCu_6$ may be on the verge of magnetic ordering and several studies at ultra-low temperatures were performed to seek for possible ordering effects. It has already been indicated by Amato *et al* [7] that the Curie–Weiss high-temperature $\chi(T)$ is followed down to $T \simeq 9$ K for the a- and b-axes of their $CeCu_6$ crystal, then $\chi(T)$ initially becomes temperature independent below this temperature before it finally increases below 1 K. Remarkably for the c-axis $\chi(T)$ follows a Curie–Weiss law from room temperature to 80 mK which was the lowest temperature used in this study. Jin *et al* [26] observed a peak in ac susceptibility at 3 mK for polycrystalline $CeCu_6$ and along the a-axis of a $CeCu_6$ single crystal. Along the b-axis peaks were observed at 2 mK and 0.5 mK. In another study on single-crystal $CeCu_6$ a decrease in the magnitude of dc magnetization below $T \simeq 3$ mK was reported by Schuberth *et al* [27], after subtraction of a baseline of what was established as a very low concentration of Gd^{3+} impurity in their sample. In addition, the specific heat C/T which was measured down to 11 mK revealed a significant upturn (to $\simeq 2800$ mJ mol^{-1} K^{-2}) below 40 mK which, considered together with the magnetization behaviour, was ascribed to possibly being the high-temperature side of a magnetic anomaly. Pollack *et al* [28] reported that at $T \simeq 1$ mK the nuclear quadrupole intensity exhibits a peak with a thermal-hysteretic character. The authors discussed the possibility that $CeCu_6$ may order unconventionally in its electronic spin system (e.g. superconducting, small-moment antiferromagnetic or spin-glass) or in its nuclear spin system at this temperature.

Doping experiments in which Ce is replaced received considerable attention. The effects of replacing Ce with non-magnetic M = La, Y or Th were investigated through specific heat measurements on polycrystalline $(Ce_{1-x}M_x)Cu_6$ alloys [29]. The evolution from dense Kondo lattice to incoherent single-ion Kondo behaviour has been studied in detail down to millikelvin temperatures for single-crystal alloys $(Ce_{1-x}La_x)Cu_6$ through electrical transport [9, 30, 31], specific heat [32] and susceptibility [31] measurements. Several studies are reported on the effect of substituting Ce with moment-bearing rare-earth ions R = Gd [33, 34], Tb [35] or

Pr [29, 36]. One would expect these studies to underscore the competition between Kondo and RKKY interactions [37]. However, although some evidence for magnetic or spin-glass ordering exists in these $(Ce_{1-x}R_x)Cu_6$ samples at low temperatures [33, 35, 36], the resistivity and magnetoresistivity are dominantly characteristic of that of a single-ion Kondo system [34].

In the present paper studies on substituting moment-bearing rare-earth elements for Ce in $CeCu_6$ are extended to include the magnetic element Nd. The compound $NdCu_6$ is characterized by magnetic ordering at $T_N = 5.9$ K [38]. The magnetic structure is complex [39] and while satellite reflections observed in neutron diffraction measurements indicate an antiferromagnetic type of ordering, some controversy exists [40] over details of the magnetic structure. Anomalous behaviour is found in susceptibility and magnetization measurements of $NdCu_6$ and a strong magnetocrystalline anisotropy is evident from a metamagnetic behaviour [38]. The metamagnetic behaviour is also reflected in $\rho(T)$ and in magnetoresistance measurements. At room temperature, $NdCu_6$ has a unit-cell volume of 414.503Å^3, which represents a $\sim$1.4% contraction of the isostructural, 420.286 Å^3 unit cell volume of $CeCu_6$ [4].

In our investigation the evolution from Kondo lattice to single-ion Kondo behaviour with increased Nd concentration is studied through $\rho(T)$ measurements on $(Ce_{1-x}Nd_x)Cu_6$ alloys. Parameters characterizing both phonon and Kondo contributions (including the Kondo temperature T_K) are extracted from the data for alloys with different x-values. We also performed magnetoresistance measurements up to 8 T and used calculations by Andrei [41] and Schlottmann [42] for the Bethe-*ansatz* solution of the Coqblin–Schrieffer Hamiltonian to analyse the results and in this way also deduce values of $T_K(x)$. The relative importance of Kondo versus magnetic behaviour will be addressed. Conference reports on parts of this study have appeared elsewhere [43, 44].

2. Experimental details

The samples were prepared by melting the constituents in an arc-furnace under argon atmosphere. Metals of purity 99.99 wt% for Ce and Nd and 99.99+ wt % for Cu were used. Room-temperature x-ray diffraction spectra for all the compounds prepared in the $(Ce_{1-x}Nd_x)Cu_6$ series could be indexed according to the expected orthorhombic *Pnma* crystal structure, and showed no detectable evidence of unreacted elements or parasitic phases. Bar-shaped specimens of typical dimensions $1 \times 1 \times 10$ mm^3 were cut by spark-erosion from the sample ingots. For electrical transport measurements, the four-probe dc method was used. Contact wires were spot-welded onto the specimens, and current- reversal was used to correct for possible thermal voltages in the circuitry.

Experimental temperatures down to $T = 1.5$ K were attained using an Oxford Instruments variable temperature insert (VTI) and superinsulated Dewar, and a superconducting solenoid matched with the Dewar and VTI provided for applied magnetic fields up to $B = 8$ T. Inside the vacuum- and radiation-shielded VTI sample space, the sample temperatures were regulated using an Oxford Instruments ITC^{503} temperature controller. We measured the sample temperatures by means of calibrated resistive carbon-glass and germanium sensors. A temperature stability of $T \pm 5$ mK could be achieved over the $\sim$20 minute duration of a $0 \rightarrow 8\,\mathrm{T} \rightarrow 0$ field-scan isotherm. Before energizing of the solenoid, control of temperature for recording an isotherm was switched from the resistive sensors to a magnetic-field-insensitive capacitance sensor using the $<$20 ppm transfer precision allowed by the temperature controller. For recording isofield data with scanning of the sample temperature, the magnetic field in persistent mode could be set and regulated to within $B \pm 1$ mT. For sample excitation current, a YEW type 2854 precision dc supply was used and the voltages were measured using a HP 3478A digital voltmeter. The electrical resistivity values $\rho(T)$ reported in this work were

measured to a sensitivity of typically 1 part in 1000. However, an absolute error of $\rho(T) \pm 2\%$ is estimated due to the uncertainty in geometrical factors. A further uncertainty in $\rho(T)$ could result from the presence of voids and microcracks in the samples and the influence of this is difficult to quantify. The effects of lattice defects on $\rho(T)$ seem to be small for these samples (see section 3.1).

3. Results and discussion

3.1. Zero-field resistivity

The temperature dependence of the zero-field resistivities $\rho(T)$ of alloys in the series $(Ce_{1-x}Nd_x)Cu_6$ is shown in figure 1. Measurements were taken at ~0.3 K temperature intervals, and the individual points therefore merge to resemble solid lines. All members of the series initially reveal a decreasing resistivity when the temperature is lowered from room temperature. A minimum in $\rho(T)$ and an upturn at low temperatures characterize all the alloys containing cerium. At the cerium-concentrated end of the series, a maximum precedes a final drop in $\rho(T)$ towards the lowest experimental temperatures (see table 1). The temperature

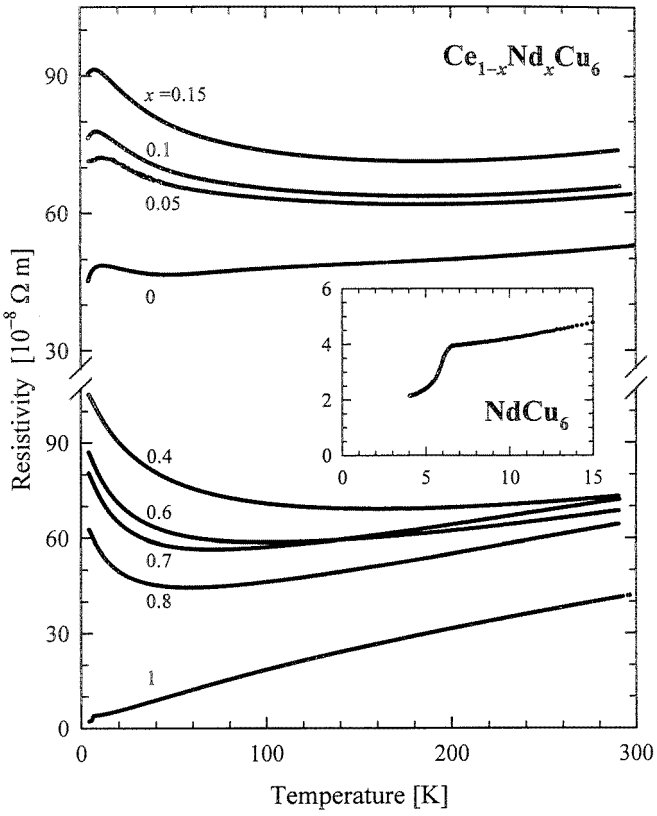

Figure 1. Temperature variation of the electrical resistivity in the range $4 \leqslant T \leqslant 295$ K for compounds in the pseudo-binary system $(Ce_{1-x}Nd_x)Cu_6$ ($0 \leqslant x \leqslant 1$). The measured data are presented as individual data points which merge to appear as solid lines, due to the small temperature intervals between the points. A negligible thermal hysteresis was detected between data collected in decreasing and subsequent increasing temperatures over the measurement range.

Table 1. The cerium-concentration dependence of extrema occurring in $\rho(T)$ for compounds in the system $(Ce_{1-x}Nd_x)Cu_6$.

x	$T(\rho = \rho_{min})$ (K)	$T(\rho = \rho_{max})$ (K)
0	47	12.2
0.05	185	11.2
0.1	182	7.9
0.15	183	7.4
0.4	162	—
0.6	100	—
0.7	70	—
0.8	59	—
1.0	—	—

where the maximum in $\rho(T)$ occurs is rapidly suppressed as the Nd content is increased. This temperature is usually associated with a Kondo lattice characteristic temperature T_0 below which phase coherence effects start to appear in the system [3, 11]. The results illustrate how with increase in Nd content a change from Kondo lattice behaviour to incoherent Kondo scattering, the latter characterized by a $-\ln T$ dependence, is obtained. The effect of antiferromagnetic order at $T_N = 6.3$ K on $\rho(T)$ of $NdCu_6$ is evident from figure 1. However, the dominant scattering in the dilute Ce region is clearly that of incoherent Kondo scattering. The $\rho(T)$ curves, for compositions and temperatures where incoherent Kondo scattering apply, may be described by

$$\rho(T) = \rho_0 + \rho_{ph}(T) - c_K \ln\left(\frac{T}{T_K}\right). \tag{1}$$

In equation (1), ρ_0 is the residual resistivity and the electron–phonon scattering term $\rho_{ph}(T)$ is often approximated as $\rho_{ph}(T) \simeq bT$. The term ρ_0 includes, in addition to the resistivity as a result of electron scattering from dislocations, grain boundaries and other lattice defects, also, as a dominant part, a Nordheim-like contribution due to atomic disorder as a result of the presence of the two kinds of rare-earth atoms (Ce, Nd) in the $CeCu_6$ lattice. Sumiyama *et al* [31] convincingly illustrated the presence of a Nordheim-like contribution for $(Ce_{1-x}La_x)Cu_6$ through resistivity measurements down to 18 mK. As indicated by these authors it reflects the saturation effects found in the magnetic resistivity $\rho_{mag}(T) = \rho(T) - \rho_{ph}(T)$ for both the dilute Kondo alloys and the Kondo-lattice system as $T \to 0$. The quantity $\rho_{mag}(T = 0)/(1 - x)$ presents the unitarity limit of resistivity ρ_U when $1 - x \to 0$ and was determined as $\rho_U = (320 \pm 30) \times 10^{-8}\ \Omega$ m for the $(Ce_{1-x}La_x)Cu_6$ system [31]. The contribution of ordinary lattice defects to ρ_0 is considerably smaller than the magnetic contribution as is evident from measurements we performed on a $LaCu_6$ sample giving $\rho(T = 4\text{ K}) = 2 \times 10^{-8}\ \Omega$ m, and on $NdCu_6$ giving $\rho(T = 4\text{ K}) = 2.1 \times 10^{-8}\ \Omega$ m. Furthermore, measurements on $CeCu_6$ down to 50 mK indicate ρ_0 values between 8 and $16 \times 10^{-8}\ \Omega$ m depending on the current direction in the single crystals used [6]. We do not expect the contribution of ordinary lattice defects to ρ_0 to vary considerably across the $(Ce_{1-x}Nd_x)Cu_6$ series since all the samples were prepared following the same procedures.

Several of the $\rho(T)$ curves in figure 1 exhibit the characteristic minimum in $\rho(T)$ at fairly high temperatures (162–185 K, see table 1) and consequently ρ_{ph} is clearly not dominant for these compounds at room temperature. Hence, to separate the Kondo and phonon terms reliably, $\rho(T)$ measurements have been extended to temperatures up to 580 K as depicted in figure 2. For purposes of clarity, data points in this figure have been depopulated so that only

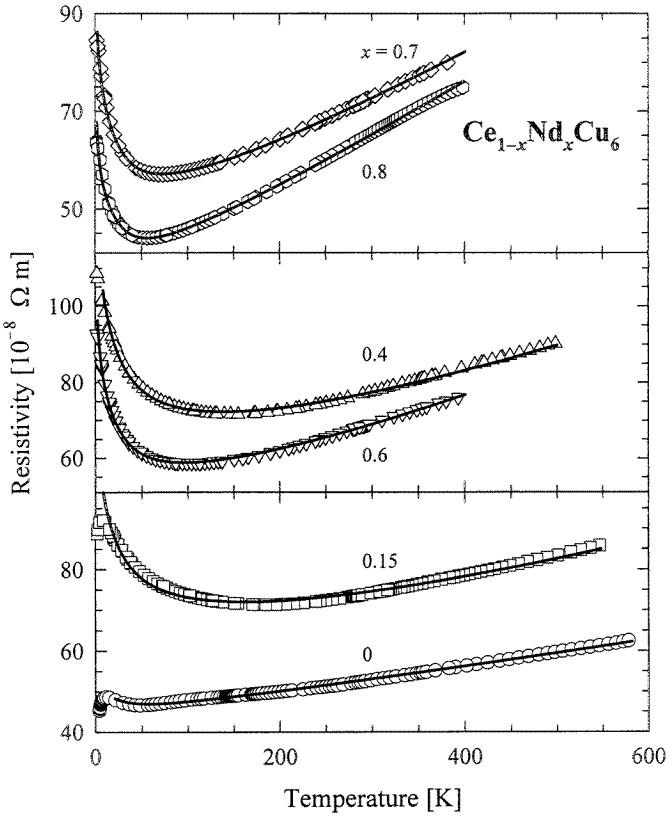

Figure 2. Temperature variation of the electrical resistivity for temperatures above $T = 1.5$ K and up to $T = 580$ K for compounds in the system $(Ce_{1-x}Nd_x)Cu_6$. The solid lines are LSQ fits of equations (1) and (2) to the data. The calculated parameters are given in table 2.

1 in every 15 measured points are shown, although for the iterated least-squares (LSQ) fitting operation discussed below, all the data were retained. In the present investigation the results for $\rho(T)$ in figure 2 are fitted to equation (1), using for the electron–phonon scattering term

$$\rho_{\rm ph}(T) = \left(\frac{4\kappa}{\theta_{\rm R}}\right)\left(\frac{T}{\theta_{\rm R}}\right)^5 \int_0^{\theta_{\rm R}/T} \frac{z^5\,{\rm d}z}{({\rm e}^z - 1)(1 - {\rm e}^{-z})}. \tag{2}$$

The Grüneisen–Bloch description [45] of the electron–phonon scattering in equation (2), while approaching the linear bT-behaviour at high temperatures, presents a more realistic description of $\rho_{\rm ph}(T)$ at low temperatures. In equation (2), κ is the electron–phonon coupling constant and $\theta_{\rm R}$ is the resistivity-characteristic Debye constant which is usually comparable to the specific heat Debye temperature $\theta_{\rm D}$. A value of $\theta_{\rm D} = 240$ K, which was derived from high-field specific heat measurements for $CeCu_6$ [46], is used in calculations involving $(Ce_{1-x}Nd_x)Cu_6$ data in this study (compare with $\theta_{\rm D} = 230$ K for $LaCu_6$ [47]). While the variation of $\theta_{\rm D}$ across the dilution series $(Ce_{1-x}Nd_x)Cu_6$ is unknown, it is not expected to vary markedly since the values of atomic masses for Nd and Ce are nearly alike, *viz.* $M({\rm Ce})/M({\rm Nd}) = 0.97$ and therefore the lattice-vibrational spectra should be similar. It is noted that the single-ion Kondo scale $T_{\rm K}$ is explicitly included in the last term of equation (1). However, we refrain from a more detailed specification of c_K or of the argument of the logarithmic term noting that a variety of descriptions exist in the literature [3]. The Kondo term in equation (1) gives an appropriate

Table 2. Least-square iteration parameter values of contributions to the electrical resistivity for the compound series $(Ce_{1-x}Nd_x)Cu_6$, obtained by fitting equations (1) and (2) to the data (see figure 2).

x	ρ_0 (10^{-8} Ω m)	κ (10^{-8} Ω m K)	c_K (10^{-8} Ω m)	T_K (K)
0.8	63 ± 2	7282 ± 11	7.37 ± 0.02	2.7 ± 0.6
0.7	76 ± 2	7017 ± 9	12.27 ± 0.02	6.8 ± 1.2
0.6	82 ± 6	6283 ± 15	12.19 ± 0.03	7.8 ± 0.4
0.4	101 ± 9	5706 ± 66	15.37 ± 0.17	9.8 ± 0.5
0.15	99 ± 3	4053 ± 20	12.45 ± 0.06	8.5 ± 1.7
0	57.5 ± 0.9	2131 ± 7	2.20 ± 0.03	0.32 ± 0.14

description for the single-ion expectation at high temperatures, but fails at low temperatures since it does not describe the saturation of the single-ion resistivity at $T \rightarrow 0$ (see [31] for saturation effects in the $(Ce_{1-x}La_x)Cu_6$ system). Finally, it is not considered necessary to include in our analyses the effects of transition-electron d-band scattering associated with the Cu atoms, since the 3d orbital of Cu is completely filled.

For all the alloys studied above room temperature, a tendency towards a linear temperature variation of $\rho(T)$ is observed at sufficiently high temperatures (see figure 2). This indicates the diminishing influence of inelastic spin-flip scattering on the total measured $\rho(T)$, and supports an interpretation whereby the high-temperature $\rho(T)$ is used to characterize, to first order, the electron–phonon scattering $\rho_{ph}(T)$. Thus, in order to resolve the various contributions to the measured $\rho(T)$, the high-temperature slopes in figure 2 were used as starting values of $\rho_{ph}(T)$ for a LSQ fit of equation (1) together with the Grüneisen–Bloch relation given in equation (2) to the $\rho(T)$ data. No high-temperature cut-off was imposed on any of the temperature-dependent terms, but a low-temperature limit was set for the LSQ fitting range of the $(Ce_{1-x}Nd_x)Cu_6$ compounds with $x \leqslant 0.4$ due to an inflection point and/or peak formation in $\rho(T)$ (see table 1). The LSQ results are illustrated as solid lines superimposed onto the respective data sets in figure 2 and the parameters are listed in table 2 and plotted against the Ce concentration in figure 3. The contribution ρ_0, the logarithmic amplitude c_K, as well as the value for the Kondo temperature T_K, reveal a maximum near $1-x = 0.6$, while the electron–phonon coupling term κ is seen to steadily diminish with decreasing Nd content. It is evident that for Nd substitutions up to $x \simeq 0.4$ atoms per formula unit, the contraction induced in the Ce sublattice causes an increase in the Kondo interaction energy, possibly due to an enhanced 4f–conduction electron hybridization (see figure 3(a)). Thus $\partial T_K/\partial V < 0$ from the initial effects of Nd substitution for Ce in $CeCu_6$. This agrees qualitatively with determinations of T_K from specific heat studies for the $(Ce_{1-x}La_x)Cu_6$ system where a monotonic and almost linear decrease of T_K with La substitution was observed [32]. Since La substitution gives a volume increase in the unit cell, it follows that $\partial T_K/\partial V < 0$ also in this case. For higher Nd concentrations the Kondo temperature T_K is seen to decrease, which is likely due to an increasingly forceful f–f indirect RKKY interaction mediated by the conduction electrons. The maximum in $\rho_0(x)$ on the other hand reflects the Nordheim-like origin of this term, $\rho_0 \sim x(1-x)$ which has a maximum at $x = 0.5$ [48].

The analysis thus far ignores, for simplicity and due to a lack of development in the theory, any cerium intersite interactions which may prevail especially in the Ce-concentrated members of the $(Ce_{1-x}Nd_x)Cu_6$ series (the magnetic ordering observed in pure $NdCu_6$ and further analysis thereof falls outside the scope of this work). In spite of this, the single-ion Kondo description embodied in equation (1) renders a fair description of the interaction of

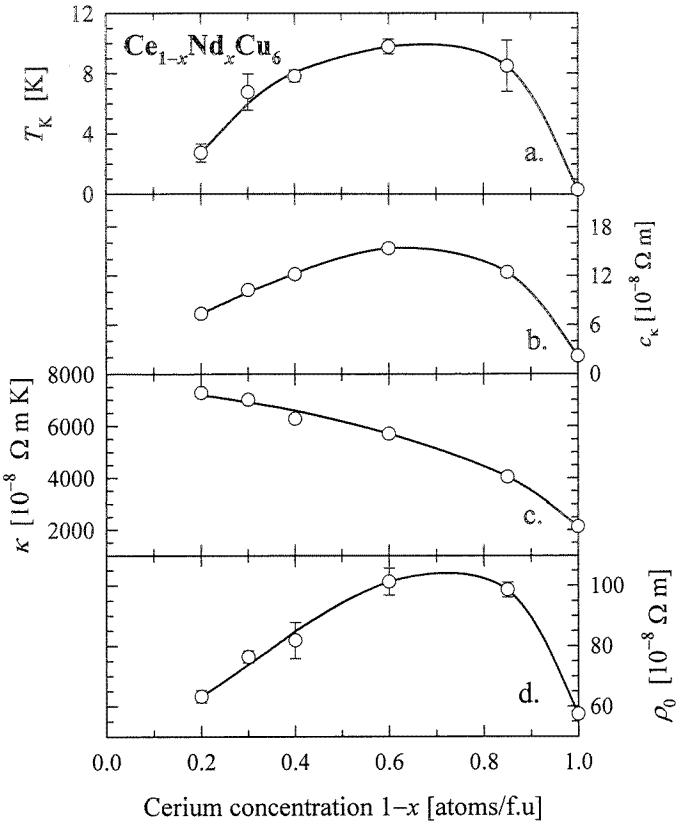

Figure 3. The calculated least-squares (LSQ) values of the Kondo temperature T_K (a), ln T-amplitude c_K (b), electron–phonon coupling constant κ (c) and the temperature-independent term ρ_0 (d) (see equations (1) and (2)) plotted against the Ce concentration for compounds in the system $(Ce_{1-x}Nd_x)Cu_6$, pertaining to data analyses illustrated in figure 2. The solid lines are a guide to the eye.

conduction electrons with the cerium magnetic centres in this system. Figure 2 illustrates the finding that even 20% Ce in $NdCu_6$ results in the incoherent Kondo interaction dominating the temperature dependence of electrical resistivity.

Deviations from the theoretical prediction of equation (1) occur at low temperatures towards the cerium-concentrated limit (see figure 2), and these may be attributed in general to cooperative effects which become significant as the thermal energy of the system is removed. Translational coherence is such a low-temperature effect which is associated with a Kondo lattice, and this is seen to be rapidly suppressed by the introduction of Nd into $CeCu_6$ (table 1). In the region of low Ce concentrations ($1 - x = 0.2$–0.6), the resistivity increases towards low temperatures without levelling off. Evidently, measurements extending to well below the presented temperature range are called for before attempting to unambiguously characterize the ground state of these alloys. As the system approaches the ground state, either the local Ce-moment must become fully screened to limit the $T \rightarrow 0$ resistivity to the unitarity limit ρ_U, or if the Ce moments remain underscreened one can expect translational coherence between these moments plus the possibility of magnetic ordering to determine the dynamics of the ground state. A qualitative description of a Kondo lattice system was given by Yoshimori and

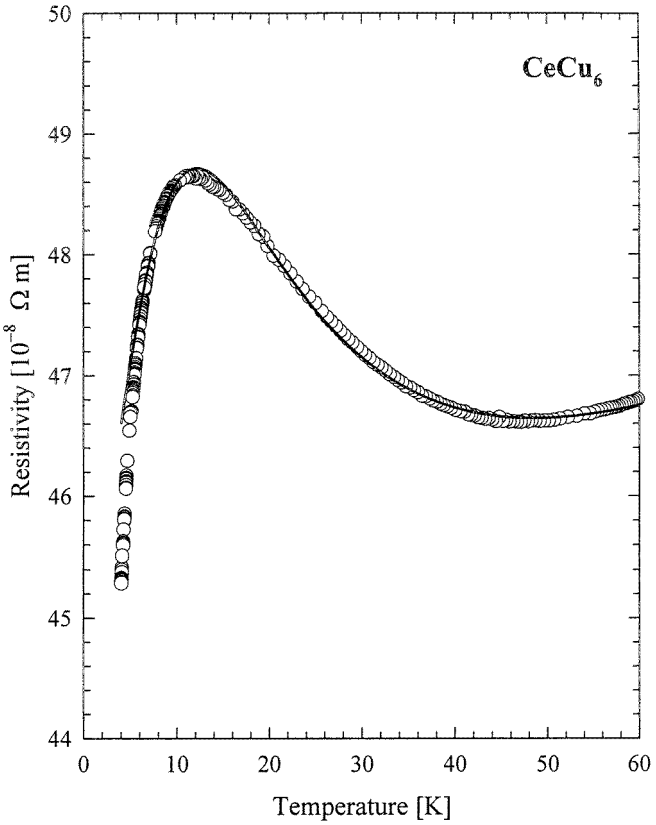

Figure 4. Temperature dependence of the electrical resistivity of CeCu6, together with a theoretical prediction due to Yoshimori and Kasai [49] (solid line) given in equation (3) and with LSQ parameters as given in the text.

Kasai [49] in the framework of the periodic Anderson model. Intersite magnetic interactions are explicitly ignored and the temperature dependence of the magnetic resistivity is calculated as

$$\rho(T) = A\left\{\left[\sqrt{\log^2\left(\frac{T}{T_K}\right)} + \frac{3\pi^2}{4} + \log\left(\frac{T}{T_K}\right)\right]^2 + \gamma\left[\sqrt{\log^2\left(\frac{T}{T_K}\right)} + \frac{3\pi^2}{4} - \log\left(\frac{T}{T_K}\right)\right]^2\right\}^{-1}. \quad (3)$$

The solid line depicted in figure 4 is the LSQ result of fitting equation (3), plus a temperature-independent ρ_0 as well as the Grüneisen–Bloch electron–phonon scattering variation $\rho_{ph}(T)$ previously calculated for $CeCu_6$ (see table 2), to the $\rho(T)$ data for $CeCu_6$. A value of $T_K \pm (0.022 \pm 0.002)$ K is calculated which is smaller than $T_K = (0.32 \pm 0.14)$ K obtained from the above single-ion Kondo analysis of the data in figure 2. The LSQ values for the other free parameters in equation (3) are $\rho_0 = (44 \pm 3) \times 10^{-8}\ \Omega$ m, $A = (147 \pm 10) \times 10^{-8}\ \Omega$ m and $\gamma = (116 \pm 2)$.

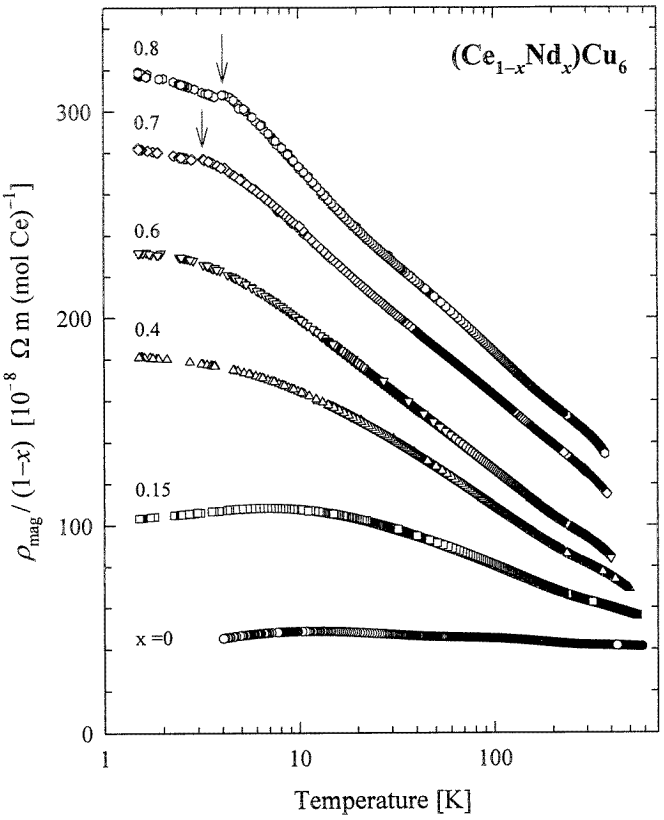

Figure 5. Temperature variation, on a $\log_{10} T$ scale, of the 4f-derived Ce-molar electrical resistivity $\rho_{\mathrm{mag}}(T)/(1-x)$ for various compounds in the system $(Ce_{1-x}Nd_x)Cu_6$ (see equation (4)). The arrows indicate the temperature of magnetic ordering, which is observed as a distinct break in the slope of $\rho_{\mathrm{mag}}(T)$ for $(Ce_{0.2}Nd_{0.8})Cu_6$ ($T_N = 4$ K) and $(Ce_{0.3}Nd_{0.7})Cu_6$ ($T_N = 3.2$ K).

To further clarify the Kondo scattering in $(Ce_{1-x}Nd_x)Cu_6$, consider the magnetic resistivity

$$\rho_{\mathrm{mag}}(T) \simeq \rho(T) - \rho_{\mathrm{ph}}(T) \tag{4}$$

which is illustrated in molar form $\rho_{\mathrm{mag}}(T)/(1-x)$ in figure 5. $\rho(T)$ is the measured resistivity, $\rho_{\mathrm{ph}}(T)$ is the Grüneisen–Bloch temperature variation of electron–phonon scattering parametrized for each compound in table 2, and $1-x$ is the Ce molar concentration. Figure 5 explicates the logarithmic temperature dependence over a wide range of temperature and Ce concentration. At the lowest cerium concentration, the magnetic resistivity reaches a value which is of the order of the unitarity limit $\rho_{\mathrm{U}} \simeq (320 \pm 30) \times 10^{-8}\ \Omega\,\mathrm{m}$ observed by Sumiyama *et al* [31].

A break in the slope is evident for the molar electrical resistivity curves for compounds with $x = 0.8$ and 0.7 in figure 5. This is interpreted as a signature of magnetic or spin-glass ordering for $(Ce_{1-x}Nd_x)Cu_6$ samples with $x \geqslant 0.7$. No evidence of such ordering was however observed for samples with $x \leqslant 0.6$. For $(Ce_{1-x}Gd_x)Cu_6$ evidence for magnetic ordering exists for $x \geqslant 0.25$ [33] and for $(Ce_{1-x}Tb_x)Cu_6$ for $x \geqslant 0.68$ [35]. Hence, $\rho(T)$ is even more dominantly of single-ion Kondo character in the $(Ce_{1-x}Nd_x)Cu_6$ system than is the case for $(Ce_{1-x}Gd_x)Cu_6$ and $(Ce_{1-x}Tb_x)Cu_6$.

3.2. Magnetoresistivity

Figure 6 displays the temperature dependence of resistivity measured respectively in zero field and in an applied field $\mu_0 H = B = 7.7$ T for a number of $(Ce_{1-x}Nd_x)Cu_6$ alloys. A negative magnetoresistivity defined as MR $= \{\rho(T, B) - \rho(T, 0)\}/\rho(T, 0)$ is observed in all cases for $T \leqslant 25$ K. For the $x = 0.15$ compound, the zero-field $T = 7$ K peak is shifted up in temperature to $T = 10$ K while for $x = 0.4$, an applied field of 7.7 T results in a maximum in $\rho(T)$ near 4 K, which suggests the development of phase coherence between semi-screened magnetic moments at lower temperatures [41]. At low temperatures the magnetic field has the greatest effect on resistivity in the cerium-concentrated alloys. The application of a magnetic field appears to have qualitatively the same effect as lowering the temperature of the system. The resonant part of electron scattering is being frozen in both cases since the ground state singlet becomes less polarizable. At higher temperatures $T \geqslant 30$ K, the observed MR is negligible.

In order to investigate the field dependence of resistivity, its response to a varying applied magnetic field at a constant temperature was measured. Figure 7 illustrates isotherms obtained in this manner. The dependent variable is chosen as $\rho(T, B)/\rho(T, 0)$. The effect of an applied field on the resistivity of $(Ce_{1-x}Nd_x)Cu_6$ clearly increases with lowering temperatures as is

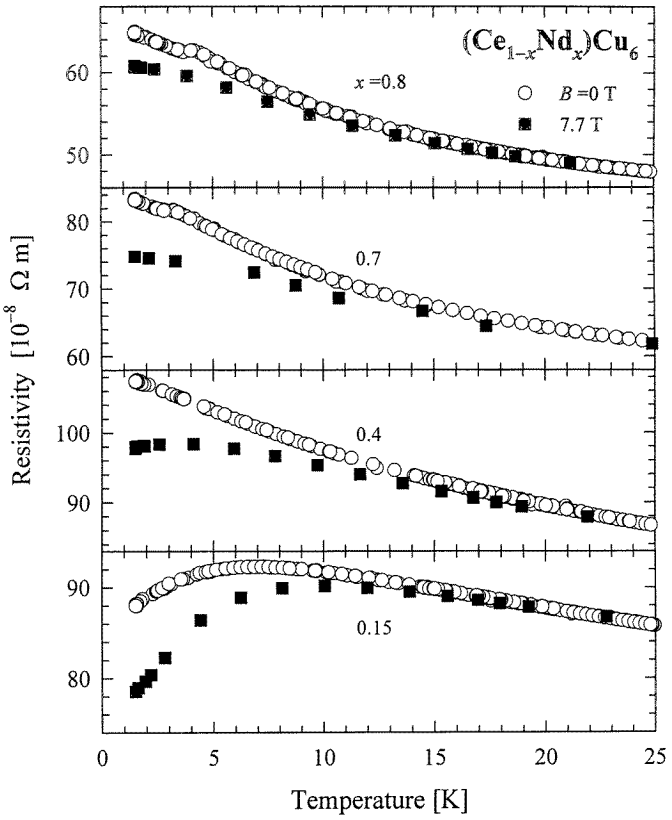

Figure 6. The temperature variation of electrical resistivity in zero field (○ symbols) and in $B = 7.7$ T (■ symbols) for compounds with $x = 0.15$, 0.4, 0.7 and 0.8 in the system $(Ce_{1-x}Nd_x)Cu_6$.

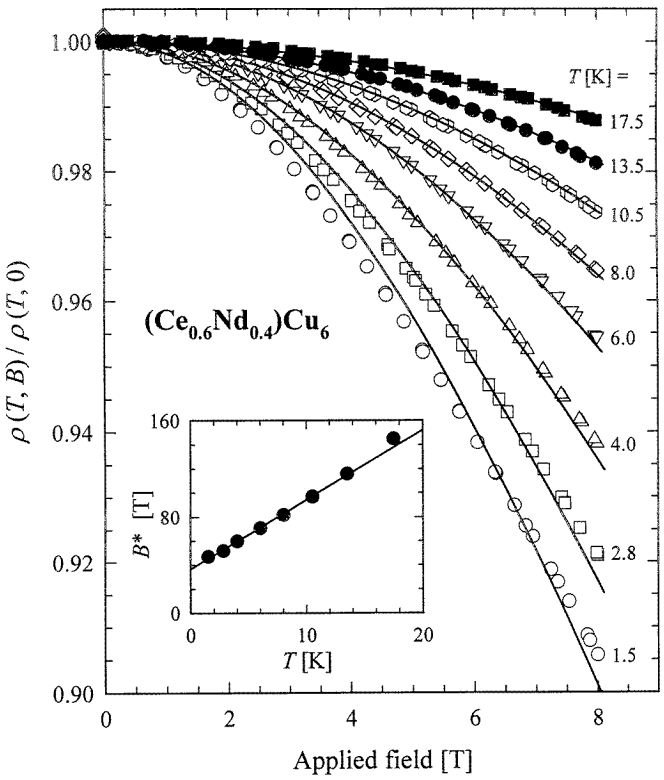

Figure 7. The isothermal magnetic-field variation of electrical resistivity at a number of sample temperatures for the representative compound $(Ce_{0.6}Nd_{0.4})Cu_6$. The data have been measured in increasing and in subsequent decreasing fields and no magnetic hysteresis could be detected. The solid lines in the main figure are LSQ fit results of the Bethe-*ansatz* theory of magnetoresistivity (see text description and equation (6)). The temperature dependence of the characteristic field $B^*(T)$ is plotted in the inset (● symbols) and LSQ fitted (solid line) against a linear function of temperature (see equation (8)) to yield various parameters that are illustrated in figure 9.

also the case with increasing cerium content, see figure 8. It is observed in figure 8 that whereas compounds with $x = 0.15$ and 0.4 exhibit a smooth dependence of resistivity on field this is not the case for the $x = 0.8$ composition. This presumably indicates that effects due to magnetic order are present in this compound at low temperatures. In pure single-crystalline $NdCu_6$ at $T = 1.3$ K, $B = 8$ T, a value of MR = +4% is measured [39] for the field parallel to either the *b*- or *c*-axis. In higher fields the magnetocrystalline anisotropy becomes more severe. The shape of $\rho(T, B)/\rho(T, 0)$ for the $x = 0.8$ composition at $T = 1.5$ K shown in figure 8 presumably originates from the superposition of a negative MR imparted by the prevailing Kondo interaction and positive contribution due to magnetic ordering which is averaged over the crystallographic directions.

The solid lines superimposed on the measured data points in figure 7 are the results of an analysis of magnetoresistivity following the calculations by Andrei [41] and Schlottmann [42] for the Bethe-*ansatz* solution of the Coqblin–Schrieffer Hamiltonian. The impurity Kondo magnetization integral [42] leads in the Bethe-*ansatz* approach to the relative 4f-level occupation due to Zeeman splitting in an applied field, as well as to the quantity $\rho(T, B)/\rho(T, 0)$. Once the temperature-scaled thermal population of the impurity level is

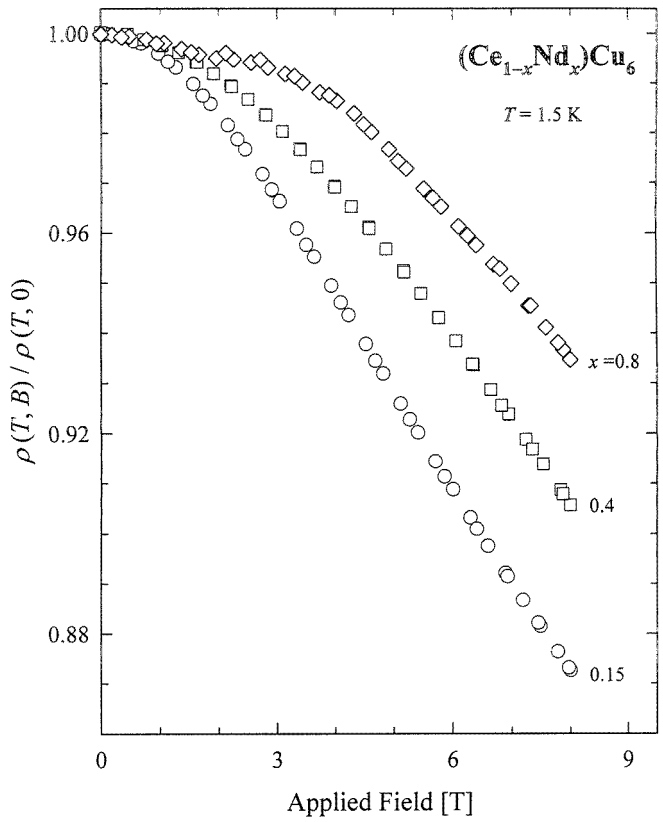

Figure 8. The $T = 1.5$ K isothermal magnetic-field variation of electrical resistivity for $(Ce_{1-x}Nd_x)Cu_6$ compounds with $x = 0.15$, 0.4 and 0.8. The data measured in increasing and in subsequent decreasing fields are shown.

known together with the field-scaled population of excited levels as a function of applied magnetic field, the magnetoresistance for the Kondo model can be calculated via the scattering phase shift [41].

For the Coqblin–Schrieffer class of Hamiltonians both the impurity magnetization M_i and magnetoresistivity as given by Friedel's sum rule can be expressed in terms of the occupation numbers n_ℓ of the f levels. It is appropriate to consider the solution for total angular momentum $j = 1/2$ for which an exact solution exists [42] although the free Ce^{3+} ion has $j = 5/2$. This is on account of the crystal-electric-field splitting which, for the orthorhombic symmetry of the $CeCu_6$ crystal, results in an effective $j = 1/2$ moment as the ground state for the Ce ions [50, 51]. Thus for $j = 1/2$, one obtains

$$M_i = \sum_{\ell=0}^{2j} (\ell - j) n_\ell \tag{5}$$

and

$$\rho(0)/\rho(B) = \frac{1}{2j+1} \sin^2 \frac{\pi n_f}{2j+1} \sum_{\ell=0}^{2j} \sin^{-2}(\pi n_\ell) \tag{6}$$

where n_f gives the f-electron occupation. The integer-valence limit of the Coqblin–Schrieffer approach to the degenerate Anderson model ($n_f \to 1$) is obtained by suppressing charge

fluctuations, thus constraining the level occupation used in equation (6) and the splitting of the $(2j + 1)$ multiplet in a magnetic field as follows

$$\sum_{\ell=0}^{2j} n_\ell = n_\mathrm{f} = 1. \tag{7}$$

In order to find $\rho(B)/\rho(0)$ we calculated the impurity magnetization numerically using expressions by Andrei *et al* [52] valid for various field regions.

The exact zero-temperature solutions for $j = 1/2$ and $j = 1$ indicate that $\rho(B)/\rho(0)$ is completely determined by a single parameter, the characteristic field B^* [42]. For finite temperatures, B^* depends on temperature and a linear relation has been indicated by Batlogg *et al* [53]

$$B^*(T) = B^*(0) + \frac{k_\mathrm{B}T}{g\mu_\mathrm{K}} = \frac{k_\mathrm{B}}{g\mu_\mathrm{K}}(T_\mathrm{K} + T) \tag{8}$$

where g is the Landé factor and the μ_K is the effective magnetic moment of the Kondo ion and T_K is the Kondo temperature.

The experimentally observed data have been LSQ-fitted against the theoretical expressions with the fits given as solid lines in figure 7. The inset shows that the characteristic field B^* depends linearly on T to a good approximation. As can be seen from fits to the isotherms, this theory gives a reasonable description of the measurements. Towards the lowest temperature studied however, the Bethe-*ansatz* prediction progressively deviates from the data. This may signal the importance of low-temperature electron scattering mechanisms other than that of the single-ion Kondo interaction. It is noted that this description of the magnetoresistivity ignores the field effect on non-elastic potential scattering which should be positive, and there is furthermore no provision made for possible interaction effects between the localized Ce magnetic moments.

The calculated parameters pertaining to the Bethe-*ansatz* description of the single-ion magnetoresistivity for the compounds with $1 - x = 0.2$, 0.3, 0.4, 0.6 and 0.85 are collected in figure 9. The indicated errors originate in the combined uncertainty from fitting equations (6) and (8) to the data. It is noted that for the Nd-rich compounds with $1 - x = 0.2$ and 0.3, equation (6) was not fitted to the MR isotherms in which evidence of magnetic ordering (below 6 K and 4 K respectively) were found. Similar to the zero-field results, the Kondo temperature initially increases upon Nd substitutions for up to $x \simeq 0.6$, but a further increase in the Nd content is observed to weaken the Kondo interaction. The observed trend in T_K with Nd substitution as well as the MR-derived magnitudes of T_K are in reasonable agreement with the findings of the single-ion analyses of zero-field electrical resistivity (figure 3). An increase in the effective cerium paramagnetic moment was reported for increasing Gd [33] or Pr [29] substitution for Ce in $CeCu_6$. A Bethe-*ansatz* analysis of MR measurements for polycrystalline $CeCu_6$ [34] revealed a Kondo moment of $\mu_\mathrm{K} = 0.2\,\mu_\mathrm{B}$. This value is only ~8% of the value of the effective high-temperature paramagnetic moment value of $\mu \simeq 2.54\,\mu_\mathrm{B}$ [7] and reflects the Kondo screening of the local Ce moments in $CeCu_6$ as the temperature is reduced. The values of μ_K that are depicted in figure 9 for compounds of $(Ce_{1-x}Nd_x)Cu_6$ are about 4% of the value of the $CeCu_6$ high-temperature paramagnetic moment.

The analysis of MR results in terms of the Bethe-*ansatz* solution supports the concept of a universal scaling of the field dependence of magnetoresistivity of single-ion Kondo systems. In figure 10(a) the isothermal magnetoresistance data for $(Ce_{0.6}Nd_{0.4})Cu_6$ are plotted against $B/B^*(T)$, using the LSQ values of $B^*(T)$ (see inset, figure 7) and data at temperatures $1.5 \leqslant T \leqslant 35$ K. Most of the isotherms are superimposed onto each other, as the Bethe-*ansatz* scaling of magnetoresistivity predicts. Towards low temperatures, however, an increasing

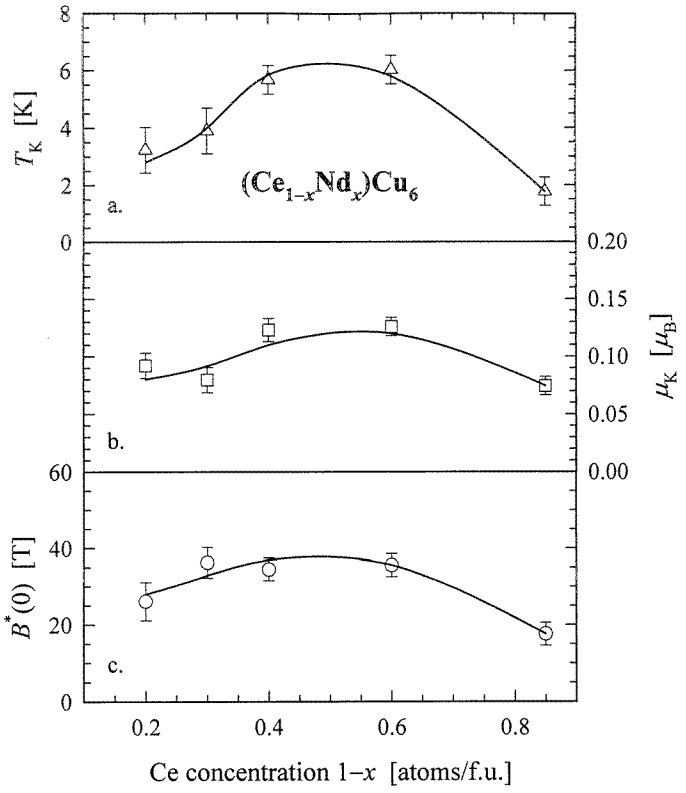

Figure 9. The Ce-concentration dependence of LSQ parameters for $(Ce_{1-x}Nd_x)Cu_6$ compounds: The Kondo temperature T_K (a), Kondo moment μ_K (b) and the characteristic Kondo field $B^*(T = 0\ K)$ (c) resulting from the Bethe-*ansatz* magnetoresistivity analyses (see equations (6) and (8) and figure 7). The solid lines are a guide to the eye.

deviation from the universal scaling relation becomes evident. This is presumably due to the development of non-single-ion coherence effects. Kondo behaviour as well as the low-temperature approach to the coherent state were recently investigated within the context of a two-channel Anderson lattice by Anders *et al* [54]. The Kondo lattice is theoretically approximated by considering an effective f site within the composite field of the lattice. It was earlier observed [55] that the experimental data of the heavy-fermion system UBe_{13} scale according to

$$\frac{\rho(T, B) - \rho(T, 0)}{\rho(T, 0)} = F\left[\frac{B}{(T^* + T)^\beta}\right]. \tag{9}$$

Motivated by this result, Anders *et al* showed that their numerical results also scale in accordance with equation (9) with the temperature $T^* = 0.006T_K$ and $\beta = 0.39$. In the impurity case these parameters are expected to take on the values $T^* = 0$ and $\beta = 1/2$ [54]. In figure 10(b), MR data for $(Ce_{0.6}Nd_{0.4})Cu_6$ are plotted against $B(T + T^*)^{-\beta}$ using isotherms with $T \leqslant 4$ K and with the values $T^*/T_K = (0.1 \pm 0.03)$ and $\beta = (0.3 \pm 0.02)$. It is noted that our fitted value of T^*/T_K for $Ce_{0.6}Nd_{0.4}Cu_6$ is an order of magnitude greater than that given by Anders *et al*. The MR data that were measured at higher temperatures, i.e. $T \geqslant 6$ K, deviate significantly from the clustering of the three isotherms shown in figure 10(b). The scaling relation in equation (9) is intended for temperatures well below T_K, where phase

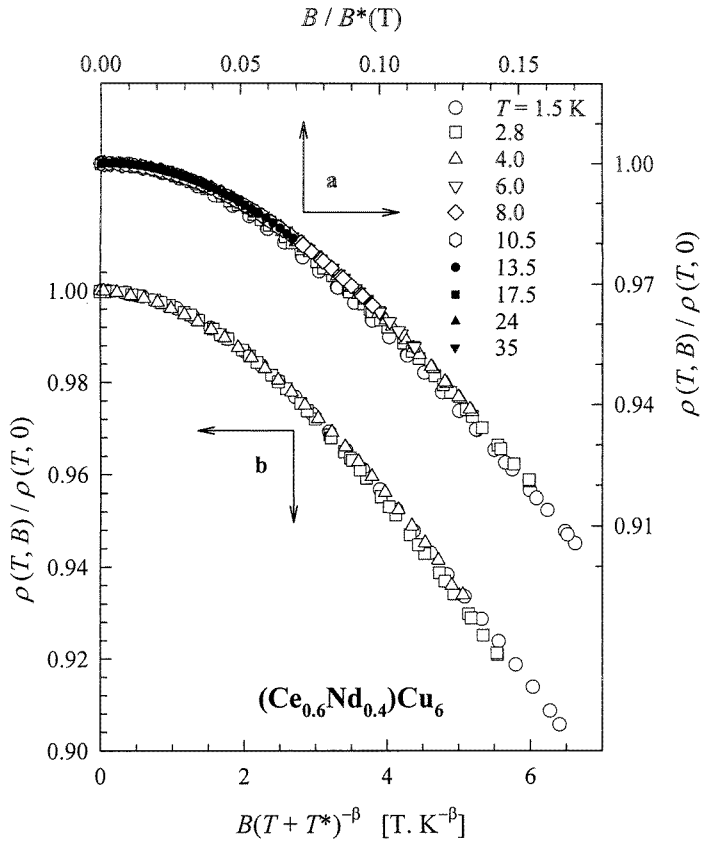

Figure 10. Scaling of magnetoresistivity data for different isotherms as measured in fields up to 8 T is compared in (a) with the Bethe-*ansatz* formulation of the single-ion magnetoresistivity and in (b) with the two-channel Anderson lattice scaling relation. The presentation of data in (a) is an alternative form of the presentation in figure 7. Universal single-ion scaling over a wide range of isotherms is followed in (a), but data at the lowest temperatures scale better to a two-channel Anderson lattice relation as indicated in (b).

coherence sets in and the Fermi-liquid ground state develops. That scaling is observed for the low-temperature isotherms, imply that some of the dynamics associated with the fully compensated Fermi-liquid ground state, such as the lifting of degeneracy that is partially achieved by applying a magnetic field, are already evident in the $(Ce_{0.6}Nd_{0.4})Cu_6$ compound in the vicinity close to and below 4 K. Comparing figures 10(a) and (b), it is evident that at low temperatures ($T \leqslant 4$ K) equation (9) provides a more accurate scaling hypothesis for the $(Ce_{0.6}Nd_{0.4})Cu_6$ magnetoresistivity isotherms than the Bethe-*ansatz* prediction.

4. Conclusions

Various effects of diluting Ce with Nd in $CeCu_6$ have been demonstrated and discussed using the temperature ($1.5 \leqslant T \leqslant 550$ K) and magnetic-field ($B \leqslant 8$ T) dependence of electrical resistivity ρ. The Kondo screening mechanism that operates on cerium 4f moments is evident in $\rho(T)$ for the substitutional series $(Ce_{1-x}Nd_x)Cu_6$. The behaviour is characteristic of an assembly of isolated magnetic ions and the single-ion description adequately accounts for the

overall features in $\rho(T)$. The Kondo interaction survives below room temperature even in the presence of a high concentration of Nd ions without any apparent effects of interactions among ions of Ce, or of Ce with Nd. Long-range magnetic ordering associated with $NdCu_6$ appears when Nd is sufficiently concentrated, but it seems to have little effect on the parameters which characterize the single-ion Kondo interaction.

The cooperative effects which appear below the Kondo lattice characteristic temperature $T_0 \sim 10$ K in $CeCu_6$ are very sensitive to Ce dilution with Nd. As the transition in $\rho(T)$ to the coherent regime is displaced to lower temperatures with increasing Nd content, the single-ion Kondo behaviour becomes valid down to even lower temperatures. On the other hand, the effect of an applied magnetic field on $\rho(T)$ for a given compound is to mimic a growth of the coherent regime and an apparent increase in the value of T_0.

The analyses of resistivity and magnetoresistivity data for the $(Ce_{1-x}Nd_x)Cu_6$ series indicate the expected reduction of the Kondo moment ($\mu_K \sim 0.1\,\mu_B$) from the high-temperature free-ion moment. The increase of T_K with initial Nd substitution is qualitatively in agreement with the decrease in T_K observed when La is substituted for Ce in $CeCu_6$, since in the Nd case the lattice volume is decreased and in the La case it is increased.

The observed transport properties indicate an evolution from the phase-coherent Kondo system, through single-ion Kondo behaviour to a magnetically ordered system as Nd is substituted for Ce. It would be desirable also to make use of other experimental methods to verify and characterize the apparent magnetic properties for large Nd substitutions. It is of interest that the $\rho(T)$ results for the $(Ce_{0.6}Nd_{0.4})Cu_6$ compound exhibit a linear temperature dependence for $1.4\ \text{K} \leqslant T \leqslant 10$ K, reminiscent of many non-Fermi-liquid materials [25, 56]. This behaviour may reflect that the system exhibits a quantum critical behaviour as a magnetic phase transition is driven to $T = 0$ K in a composition of appropriate Ce concentration. Extension of measurements to more values of x and to lower temperatures are needed before definitive conclusions can be reached.

Acknowledgments

The South African Foundation for Research Development and the University of the Witwatersrand Research Committee are thanked for financial support. Svetlana Papian is thanked for her involvement during the initial stages of this investigation.

References

[1] Ōnuki Y, Shimizu Y and Komatsubara T 1984 *J. Phys. Soc. Japan* **53** 1210
[2] Stewart G R, Fisk Z and Wire M S 1984 *Phys. Rev.* B **30** 482
[3] Bauer E 1991 *Adv. Phys.* **40** 417
[4] Vrtis M L, Jorgensen J D and Hinks D G 1990 *J. Solid State Chem.* **84** 93
[5] Ōnuki Y, Shibutani K, Hirai T, Komatsubara T, Sumiyama A, Oda Y, Nagano H, Sato H and Yonemitsu K 1985 *J. Phys. Soc. Japan* **54** 2804
[6] Amato A, Jaccard D, Walker E and Flouquet J 1985 *Solid State Commun.* **55** 1131
[7] Amato A, Jaccard D, Flouquet J, Lapierre F, Tholence J L, Fisher R A, Lacy S E, Olsen J A and Phillips N E 1987 *J. Low Temp. Phys.* **68** 371
[8] Sato H, Zhao J, Pratt W P Jr, Ōnuki Y and Komatsubara T 1987 *Phys. Rev.* B **36** 8841
[9] Sumiyama A, Oda Y, Nagano H, Ōnuki Y and Komatsubara T 1985 *J. Phys. Soc. Japan* **54** 877
[10] Reinders P H P, Springford M, Coleridge P T, Boulet R and Ravot D 1986 *Phys. Rev. Lett.* **57** 1631
[11] Chapman S, Hunt M, Meeson P, Reinders P H P, Springford M and Norman M 1990 *J. Phys.: Condens. Matter* **2** 8123
[12] Ott H R, Rudigier H, Fisk Z, Willis J O and Stewart G R 1985 *Solid State Commun.* **53** 235

[13] Aeppli G, Yoshizawa H, Endoh Y, Bucher E, Hufnagl J, Ōnuki Y and Komatsubara T 1986 *Phys. Rev. Lett.* **57** 122
[14] Rossat-Mignod J, Regnault L P, Jacoud J L, Vettier C, Lejay P, Flouquet J, Walker E, Jaccard D and Amato A 1988 *J. Magn. Magn. Mater.* **76/77** 376
[15] Regnault L P, Erkelens W A C, Rossat-Mignod J, Jacoud J L, Flouquet J, Mignot J M, Walker E, Jaccard D, Amato A and Vettier C 1988 *J. Physique Coll.* **49** C8 773
[16] Amato A 1997 *Rev. Mod. Phys.* **69** 1119
[17] Amato A, Feyerherm R, Gygax F N, Jaccard D, Schenck A, Sierro J, Walker E and Zimmermann U 1993 *Physica* B **186–188** 273
[18] Germann A, Nigam A K, Dutzi J, Schröder A and Löhneysen H v A 1988 *J. Physique Coll.* **49** C8 755
[19] Schlager H G, Schröder A, Welsh M and Löhneysen H v 1993 *J. Low Temp. Phys.* **90** 181
[20] Pietrus T, Bogenberger B, Mock S, Sieck M and Löhneysen H v 1995 *Physica* B **206/207** 317
[21] Gangopadhyay A K, Schilling J S, Schuberth E, Gutsmiedl P, Gross F and Andres K 1988 *Phys. Rev.* B **38** 2603
[22] Fraunberger G, Andraka B, Kim J S, Ahlheim U and Stewart G R 1989 *Phys. Rev.* B **40** 4735
[23] Sieck M, Speck C, Waffenschmidt M, Mock S and Löhneysen H v 1996 *Physica* B **223/224** 325
[24] Löhneysen H v, Pietrus T, Portisch G, Schlager H G, Schröder A, Sieck M and Trappmann T 1994 *Phys. Rev. Lett.* **72** 3262
[25] Löhneysen H v 1995 *Physica* B **206/207** 101
[26] Jin C, Lee D M, Pollack L, Smith E N, Markert J T, Maple M B and Hinks D G 1994 *Physica* B **194–196** 207
[27] Schuberth E A, Schupp J, Freese R and Andres K 1995 *Phys. Rev.* B **51** 12 892
[28] Pollack L, Hoch M J R, Jin C, Smith E N, Parpia J M, Hawthorne D L, Geller D A, Lee D M, Richardson R C, Hinks D G and Bucher E 1995 *Phys. Rev.* B **52** R15707
[29] Kim J S and Stewart G R 1994 *Phys. Rev.* B **49** 327
[30] Ōnuki Y, Shimizu Y, Nishihara M, Machii Y and Komatsubara T 1985 *J. Phys. Soc. Japan* **54** 1964
[31] Sumiyama A, Oda Y, Nagano H, Ōnuki Y, Shibutani K and Komatsubara T 1986 *J. Phys. Soc. Japan* **55** 1294
[32] Satoh K, Fujita T, Maeno Y, Ōnuki Y and Komatsubara T 1989 *J. Phys. Soc. Japan* **58** 1012
[33] Roy S B, Lees M R, Stewart G R and Coles B R 1991 *Phys. Rev.* B **43** 8264
[34] Bauer E, Gratz E, Maikis M, Kirchmayr H, Roy S B and Coles B R 1993 *Physica* B **186–188** 586
[35] Radha S, Roy S B, Nigam A K, Ramakrishnan S and Chandra G 1995 *Physica* B **215** 222
[36] Roy S B, Stewart G R and Coles B R 1991 *J. Magn. Magn. Mater.* **97** 291
[37] Doniach S 1977 *Physica* B **91** 231
[38] Ōnuki Y, Ina K, Nishihara M, Komatsubara T, Takayanagi S, Kameda K and Wada N 1986 *J. Phys. Soc. Japan* **55** 1818
[39] Takayanagi S, Furukawa E, Wada N, Ōnuki Y and Komatsubara T 1990 *Physica* B **163** 574
[40] Yoshizawa H, Mitsuda S, Ōnuki Y and Komatsubara T 1986 *J. Phys. Soc. Japan* **55** 2911
[41] Andrei N 1982 *Phys. Lett.* A **87** 299
[42] Schlottmann P 1983 *Z. Phys.* B **51** 223
[43] Papian S, du Plessis P de V and Strydom A M 1996 *Physica* B **223/224** 292
[44] Strydom A M and du Plessis P de V 1998 *J. Magn. Magn. Mater.* **177–181** 413
[45] Meaden G H 1965 *Electrical Resistance of Metals* (New York: Plenum)
[46] Stewart G R, Andraka B, Quitmann C, Treadway B, Shapira Y and McNiff E J Jr 1988 *Phys. Rev.* B **37** 3344
[47] Fujika T, Satoh K, Ōnuki Y and Komatsubara T 1985 *J. Magn. Magn. Mater.* **47/48** 66
[48] Blatt F J 1968 *Physics of Electronic Conduction in Solids* (New York: McGraw-Hill)
[49] Yoshimori A and Kasai H 1983 *J. Magn. Magn. Mater.* **31–34** 475
[50] Zemirli S and Barbara B 1985 *Solid State Commun.* **56** 385
[51] Cornut B and Coqblin B 1972 *Phys. Rev.* B **5** 4541
[52] Andrei N, Furuya K and Lowenstein J H 1983 *Rev. Mod. Phys.* **55** 331
[53] Batlogg B, Bishop D J, Bucher E, Golding B Jr, Ramirez A P, Fisk Z, Smith J L and Ott H R 1987 *J. Magn. Magn. Mater.* **63/64** 441
[54] Anders F B, Jarrel M and Cox D L 1997 *Phys. Rev. Lett.* **78** 2000
[55] Andraka B and Stewart G R 1994 *Phys. Rev.* B **49** 12 359
[56] Maple M B, de Andrade M C, Herrman J, Dalichaouch Y, Gajewski D A, Seaman C L, Chau R, Movshovich R, Aronson M C and Osborn R 1995 *J. Low Temp. Phys.* **99** 223